A METHODOLOGY FOR DETERMINATION OF PIEZOELECTRIC ACTUATOR AND SENSOR LOCATION ON BEAM STRUCTURES

I. Bruant, G. Coffignal and F. Lene

Laboratoire de Modélisation et Mécanique des Structures, CNRS UPRES A 8007, 8 *rue du Capitaine Scott*, 75015 *Paris, France. E-mail: bruant@ccr.jussieu.fr*

and

M. Verge

Laboratoire d'Automatique des Arts et Métiers, ENSAM Centre de Paris, 151 *Boulevard de l'Hôpital*, 75015 *Paris, France*

In the design of actively controlled structures, the determination of the actuators and sensors location is a very important issue. In this way, the purpose of this paper is to propose a new approach to find the optimal location of piezoelectric actuators and sensors on beam structures. More precisely, first the optimization criteria are defined: it is proposed here to find the optimal actuators location by minimizing the mechanical energy integral of the system and the optimal sensors location by maximizing the energy of the state output. In the two cases, a sensitivity method applied to the discrete equations is used. Several results are presented. This methodology is used to find the optimal location of one actuator and one sensor on a cantilever beam, and on a three-beam structure. When there are different optimal locations, several performance measures are considered in order to keep one location.

1. INTRODUCTION

Recent studies on structural control systems using piezoelectric materials have shown such materials to be effective in vibration suppression of structures [1–4]. Piezoelectric materials are applied in structural vibration control to take advantage of their fast response, of their flexibility to be used as sensors and actuators in a large variety of applications, and the fact that they provide a broadband frequency response. They are lightweight and can be bonded (or embedded) to a variety of structures.

Some parameters, like location of actuators and sensors, have a major influence on the performance of the control system [5]. Many studies have been developed on optimal locations of actuators and sensors. Different cost functions and performance measures have been used. In the case of optimization of actuator location, Arbel [6], Hac [7] and Devasia [8] proposed to maximize a controllability criterion using a measure of the gramian matrix. This approach seeks to ensure active damping of all needed modes. A second usual optimization cost function is a linear quadratic optimal framework. Dhingra [9], Kondoh [10] and Yang [1] proposed a quadratic cost function taking into account the measurement error and control energy. They used it simultaneously to find optimal location of actuators

and sensors. However, the most usual performance function for sensor location uses the energy of the state output so as to maximize the information given by sensors. Baruh [11] and Hac [7] rather proposed to maximize measures of the gramian observability matrix in order to have optima without dependence on initial conditions.

In this paper, a methodology is proposed to find the actuators and sensors location to increase control efficiency. In order to simplify the optimization problem, it was decided to search independently the optimal location of actuators and that of sensors.

Consequently, it is proposed here to obtain optimal actuators location by minimizing the mechanical energy integral of the system. The optimal sensors location is found by maximizing a measure of the observability gramian. This methodology is developed here for beam structures, but it can be used for more complex structures (which is our future aim). It uses mechanical and state equations of the structure.

In section 2, we point out the active vibration control equations for beam structures. The control system is developed from a finite element modelling, and uses a linear quadratic control method including a state observer. Simulations in the case of a three-beam structure show the influence of actuators and sensors location on the control efficiency.

In section 3, we present the optimization problems of actuators location and those of sensors location. They are solved independently by using a sensitivity gradient algorithm. This method is based on the differentiation of the optimization criteria and equations of motion with respect to the design variables. The derivatives of each criterion are detailed in section 4.

Results of simulations are presented in section 5. We use the methodology to find the optimal location of one actuator and one sensor on a three-beam structure and on a cantilever beam. For some cases, the algorithm gives several optimal locations.

In order to select one location among the different best obtained placements, we propose several performance measures. In the case of the cantilever beam, we also examine the optimal location of a second actuator and a second sensor.

2. INFLUENCE OF THE ACTUATORS AND SENSORS LOCATION

2.1. MODELLING

The active vibration control of flexible elastic beam structures using piezoelectric actuators and sensors is considered. Figure 1 shows a three-beam example of such

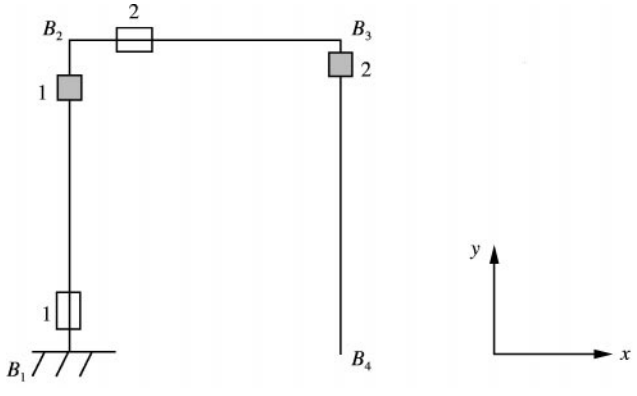

Figure 1. A three-beam structure: —■—, sensor; —□—, actuator.

a structure. Each actuator and sensor (each active device) is made up of a pair of piezoelectric materials attached symmetrically.

It is assumed that a known and representative loading condition has been previously chosen before starting the optimization process. It is not discussed here as to how to make this choice and what its influence on the optimal location of active devices is.

The finite element modelling of this kind of structure has been developed in reference [12]. One has the discrete equations

$$[K_{UU}]\{q_U\} + [K_{U\Phi}]_a\{q_\Phi\}_a + [M_{UU}]\{\ddot{q}_U\} = \{F_U\}, \tag{1}$$

$$[K_{\Phi U}]_s\{q_U\} + [K_{\Phi\Phi}]_s\{q_\Phi\}_s = \{0\}, \tag{2}$$

where $\{q_U\}$ (size $N\,ddl$), $\{q_\Phi\}_s$ (size $\bar{N}_s$) and $\{q_\Phi\}_a$ (size $\bar{N}_a$) are the generalized displacements and the generalized potentials of sensors and actuators. $[K_{UU}]$, $[M_{UU}]$, $\{F_U\}$, are the stiffness matrix, the mass matrix and the applied load vector; $[K_{U\Phi}]_a$ and $[K_{\Phi U}]_s$ couple the mechanical properties to the electric properties and $[K_{\Phi\Phi}]_s$ is the electric stiffness matrix. The subscripts a and s denote actuator and sensor. Dots indicate the derivative with respect to time.

In order to use these equations, the solution $\{q_U\}$ is decomposed into the normalized orthogonal modal basis $\{\psi_n\}$. The eigenmodes $\{\psi_n\}$ corresponding to the eigenvalues ω_n $(n = 1, \ldots, \infty)$ are solutions of the eigenproblems [13]

$$([K_{UU}] - \omega_n^2[M_{UU}])\{\psi_n\} = 0 \tag{3}$$

and satisfy the orthogonality property:

$$\begin{aligned} \{\psi_n\}^{\mathrm{T}}[M_{UU}]\{\psi_m\} &= 0, \quad n \neq m, \\ \{\psi_n\}^{\mathrm{T}}[M_{UU}]\{\psi_m\} &= 1, \quad n = m. \end{aligned} \tag{4}$$

Assuming that the contribution of the highest modes is negligible, one keeps only the first N eigenmodes,

$$\{q_U\} = \sum_{r=1}^{N} \{\Psi_r\}\alpha_r(t) = [\Psi]\{\alpha\}, \tag{5}$$

where $[\Psi]$ (size $Nddl \times N$) is the modal shape matrix.

Substituting equation (5) into equations (1) and (2) leads to the equations

$$\{\ddot{\alpha}\} + [\omega]^2\{\alpha\} = [\Psi]^{\mathrm{T}}\{F_U\} + [\Psi]^{\mathrm{T}}[K_{U\Phi}]_a\{q_\Phi\}_a,$$

$$\{q_\Phi\}_s = -[K_{\Phi\Phi}]_s^{-1}[K_{\Phi U}]_s[\Psi]\{\alpha\}.$$

As usual, these N equations can be written in a state-space form. Using the state vector (size $2N$)

$$\{x\} = \{\omega_n\alpha_n \;\; \dot{\alpha}_n\}^{\mathrm{T}} \tag{6}$$

yields

$$\frac{\mathrm{d}(x)}{\mathrm{d}t} = [A]\{x\} + [B]\{q_\Phi\}_a + \{g\}, \tag{7}$$

$$\{x\}(t=0) = \{x_0\}, \qquad \{y\} = \{q_\Phi\}_s = [C]\{x\}. \tag{8, 9}$$

The input of the system is the voltage applied to the actuators and the output is the voltage across the sensors. $[A]_{(2N,\,2N)}$, $[B]_{(2N,\,2\bar{N}_a)}$, $[C]_{(2\bar{N}_s,\,2N)}$ and $\{g\}_{(2N,\,1)}$ are the state, control output and load matrices, given by

$$[A] = \begin{pmatrix} [0] & [\omega] \\ [-\omega] & [0] \end{pmatrix} \quad [B] = \begin{pmatrix} [0] \\ [\Psi]^{\mathrm{T}}[K_{U\Phi}]_a \end{pmatrix},$$

$$[C] = \begin{pmatrix} -[K_{\Phi\Phi}]_s^{-1}[K_{\Phi U}]_s\{\Psi_r\} \\ \omega_r \end{pmatrix} [0] \Bigg), \quad \{g\} = \begin{pmatrix} \{0\} \\ [\Psi]^{\mathrm{T}}\{F\} \end{pmatrix}.$$

$\{x_0\}$ is the initial conditions vector.

2.2. CONTROL SYSTEM

In order to actively control vibrations, a linear quadratic control method, including a state observer, is used. It consists in using a control law

$$\{q_\Phi\}_a = -[K]\{\hat{x}\}, \tag{10}$$

which minimizes the cost function

$$J_\Phi = \frac{1}{2}\int_0^\infty [\{\hat{x}\}^{\mathrm{T}}[Q]\{\hat{x}\} + \{q_\Phi\}_a^{\mathrm{T}}[R]\{q_\Phi\}_a]\,\mathrm{d}t, \tag{11}$$

where $\{\hat{x}\}$ is the estimate of $\{x\}$. $\{\hat{x}\}$ is obtained with the state Luenberger observer, and is a solution of

$$\frac{\mathrm{d}}{\mathrm{d}t}\{\hat{x}\} = [A]\{\hat{x}\} + [B]\{q_\Phi\}_a + [L](\{y\} - [C]\{\hat{x}\}), \tag{12}$$

where $[L]$ is the observer gain matrix [4, 12, 14]. The choice of $[Q]$ and $[R]$ is detailed in reference [15]. Here, $[Q]$ is chosen so that $\{x\}^{\mathrm{T}}[Q]\{x\}$ represents the mechanical energy. $[R]$ is chosen such that the maximum values of $\{q_\Phi\}_a$ are less than the maximum admissible values of piezoelectric materials for the considered loads. In practice, once a maximum admissible load is chosen, several simulations are done, using different $[R]$, to select an admissible one.

2.3. SIMULATIONS

The control algorithm may be summarized by two main steps.

Step 1: the discretization of the structure using a finite composite beam element [12] and the determination of the state-space model of the system.

Step 2: the construction of the control and observer.

Step 1 has been developed in DYNADID2D [16] while step 2 has been done by using SCILAB [17] (software developed at INRIA). Each active device is discretized using several adjacent elements. Several simulations presented in references [12, 15] show the efficiency of the control system for different structures. Considered here is a three-beam structure (Figure 1) controlled by one actuator and one sensor. The geometrical and mechanical

TABLE 1

Characteristics of the three-beam structure

B_1 (m)	(0, 0)
Length B_1B_2 (m)	0·5
Length B_2B_3 (m)	0·4
Length B_3B_4 (m)	0·5
Location of actuator 1 (m)	(0, 0·02)
Location of actuator 2 (m)	(0·04, 0·5)
Location of sensor 1 (m)	(0, 0·42)
Location of sensor 2 (m)	(0·4, 0·46)
Length of each actuator (m)	0·06
Length of each sensor (m)	0·01
Natural frequencies (Hz)	1·48, 2·89, 7·99, 29·64
Width of elastic beams (m)	0·025
Thickness of elastic beams (m)	0·002
Mass density of elastic beams (kg/m^3)	2700
Young's modulus of elastic beams (Pa)	$7{\cdot}3 \times 10^{10}$

TABLE 2

Characteristics of piezoelectric PZT

Width (m)	0·01
Thickness (m)	0·001
Mass density (kg/m^3)	7440
Young's modulus (Pa)	4×10^{10}
Piezoelectric constant ε_{33}	$1{\cdot}72 \times 10^{-8}$
Piezoelectric constant d_{31} (m/V)	230×10^{-12}
Maximal admissible voltage (V)	250

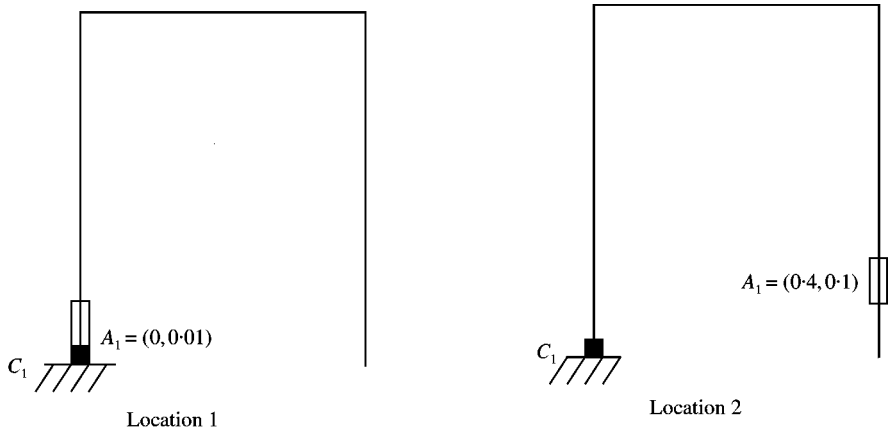

Figure 2. The two different actuator locations.

properties of the system are detailed in Tables 1 and 2. The structure is subjected to a release test derived from the load $\mathbf{F} = F\mathbf{x}$, applied at B_4 and defined as

$$\text{for } t < 0, \quad F(t) = 0{\cdot}05 \text{ N},$$

$$\text{for } t \geqslant 0, \quad F(t) = 0 \text{ N}. \tag{13}$$

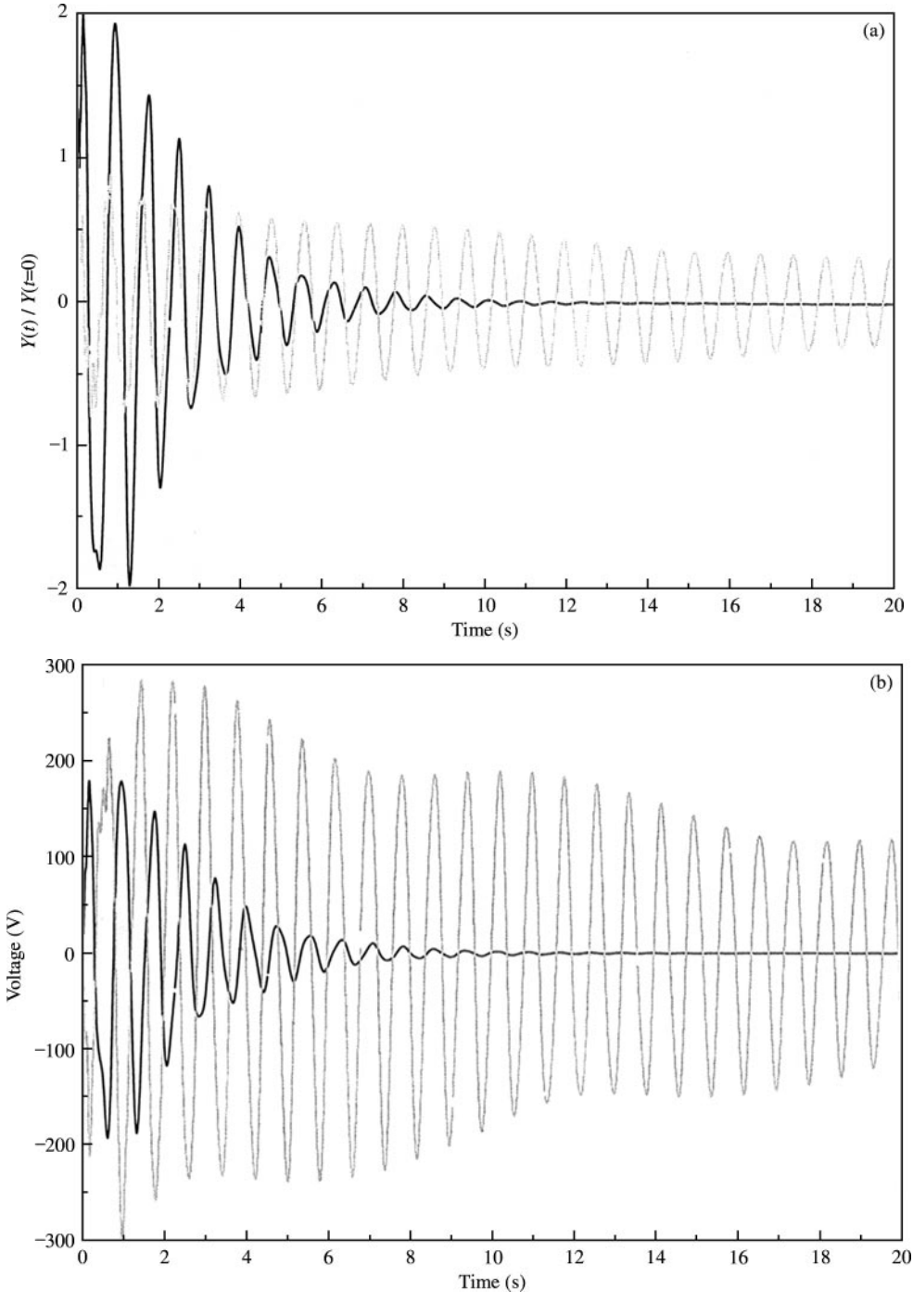

Figure 3. Influence of the actuator location. (a) Output sensor; (b) input actuator: ———, location 1; —, location 2.

Due to the nature of the excitation, only the four first eigenmodes are taken into account. The active control of this structure is detailed in reference [12]. Here, the dependence of control efficiency on actuators and sensors locations is presented.

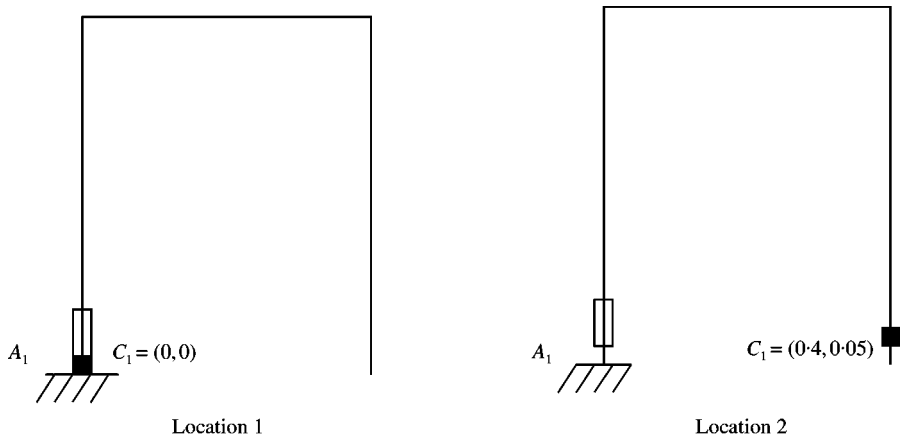

Figure 4. The two different sensor locations.

First, the sensor location is fixed at $C_1 = (0, 0)$ and two locations are considered for the actuator: $A_1 = (0, 0{\cdot}01)$ and $A_2 = (0{\cdot}4, 0{\cdot}1)$ (see Figure 2). Comparing results for both actuator locations in the case of a closed loop shows that the first location is better than the second one: the sensor output vanishes in less than 10 s whereas for the second location it requires more than 40 s. Also, the first location uses less electric energy than the second one (see Figure 3).

The influence of sensor location on the efficiency of the control can also be shown. Now, the actuator location is fixed at $A_1 = (0, 0{\cdot}01)$ and two sensor locations are considered: $C_1 = (0, 0)$ and $C_2 = (0{\cdot}4, 0{\cdot}05)$ (see Figure 4). Results for these two sensor locations, are plotted in Figure 5. At the beginning, the amplitude of the output for case 1 is higher than that for case 2: for the first location, the sensor gives better information and faster than that located at C_2. Thus, the control system reacts faster too. The maximum value of $\{q_\Phi\}_a$ in the first case is higher than that of case 2: the control is more efficient; the output decreases quickly. Consequently, the first sensor location is better than the second one.

Simulations presented for the three-beam structure illustrate the influence of actuators and sensors locations on the efficiency of active control. Some locations of the actuators may of course induce non-controllability while some locations of sensors may induce non-observability. But even if controllability and observability are maintained, the efficiency of the control can be improved by choosing better locations and shapes for sensors and actuators.

3. THE TWO OPTIMIZATION PROBLEMS

3.1. MODELLING

In order to develop a methodology for determination of actuators and sensors geometry on structures, first the design variables have to be defined to describe shape, dimensions and location. In the case of a rectangular actuator (or sensor) located on a plate, possible variables are detailed in Figure 6. In the case of a beam structure, the optimization variables can be a location a_1 and a length a_2 (see Figure 7). In the subsequent applications, beam structures, are to be considered, but the following developments can be used for more complex structures. Here, the shape of each actuator and sensor is assumed to be known and its length is constant. The only design parameter is thus an abscissa a_i.

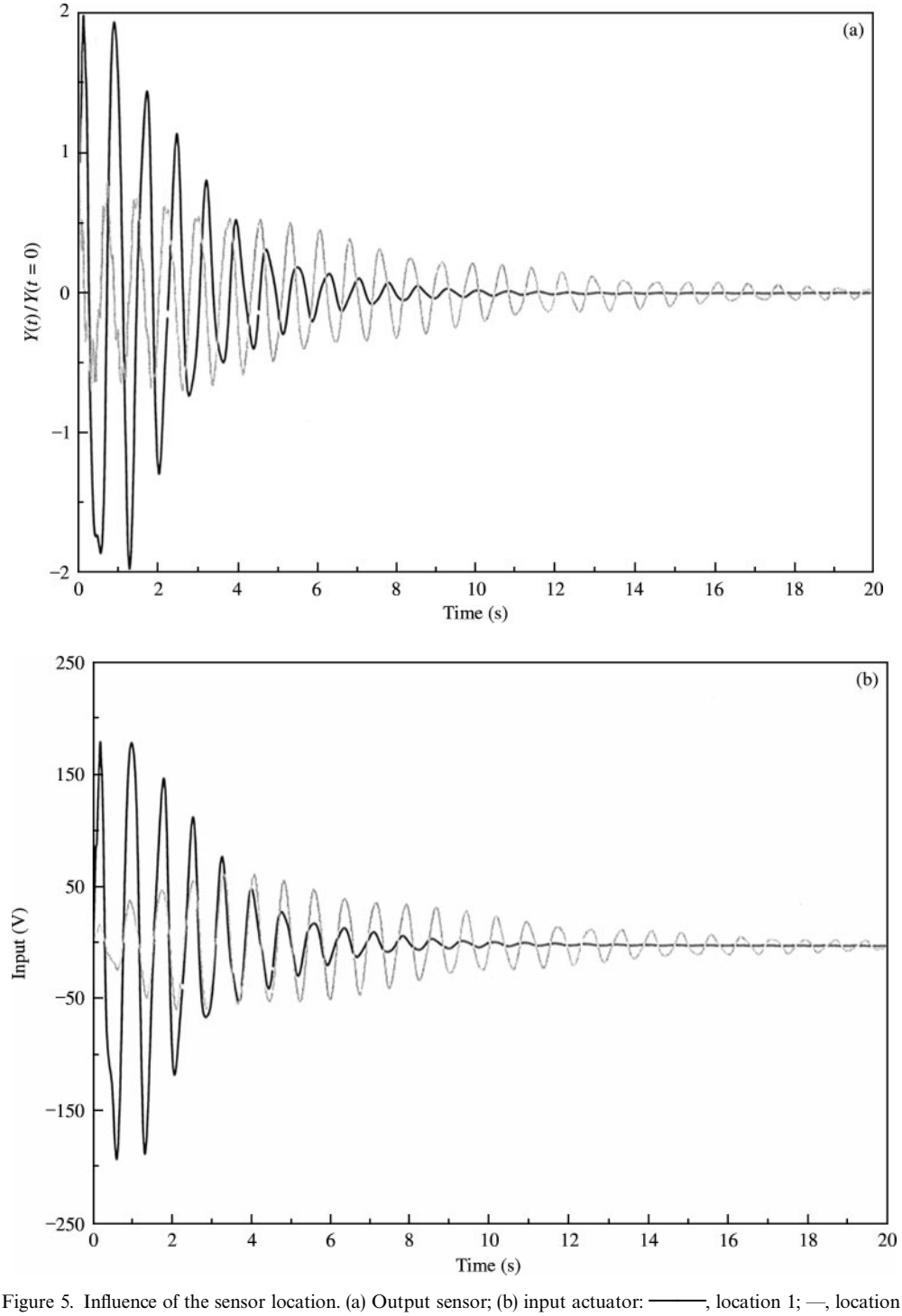

Figure 5. Influence of the sensor location. (a) Output sensor; (b) input actuator: ———, location 1; —, location 2.

To sum up, the locations of some nodes of the finite element discretization are described by a set of design parameters. As a consequence, it is straightforward to calculate derivatives of finite element matrices and vectors with respect to design parameters: they are

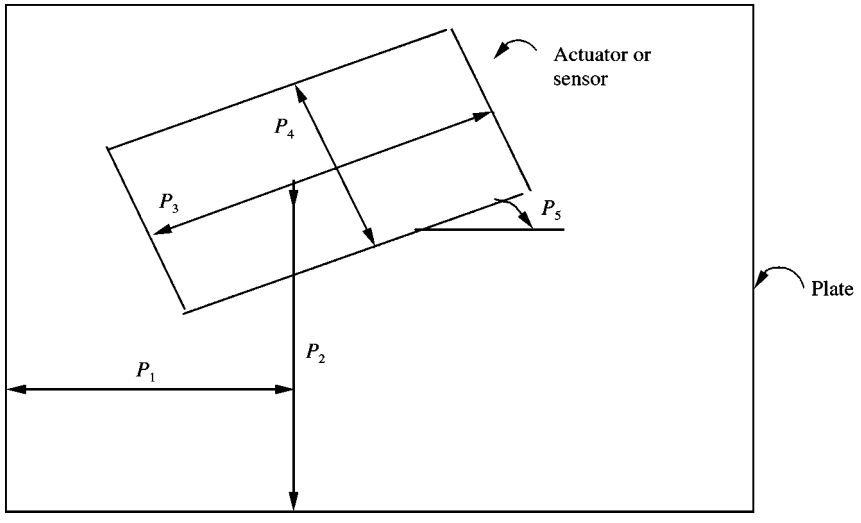

Figure 6. Design parameters in the case of plates.

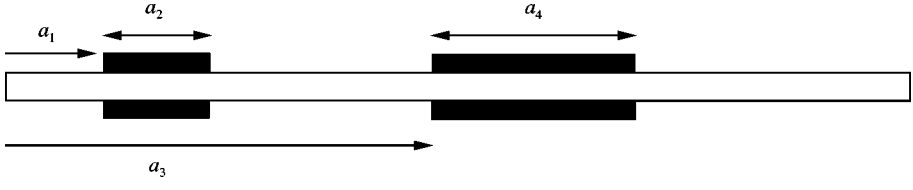

Figure 7. Design parameters in the case of beams.

combinations of derivatives with respect to node locations which can be easily and systematically calculated at the element level.

To simplify the optimization problem, first one can search independently for optimal locations of actuators and sensors, and then assume that an observer is not needed. The motivations for splitting the optimization problem into two independent ones are the following: first, practically, an optimal transmission of power (optimal location of actuator) is the priority. In another part, optimizing simultaneously the location of several active devices would necessitate dealing with a constrained optimization problem in order to avoid superposition of devices.

In practice, when using the finite element method, each active device is modelled by a set of elements. The shape of each element can be made dependent upon the location of nodes (isoparametric elements for instance). Thus, the shape of the active device may be described by the location of the nodes it is connected to. In the case considered here (see Figure 8), each active device is modelled by a set of two-node beam elements. N_L and N_R are, respectively, its left and right outer nodes.

3.2. THE OPTIMIZATION CRITERIA FOR ACTUATORS LOCATION

In the case of actuators location, as already described in the introduction, the goal is to increase control efficiency (i.e., suppress vibrations as quickly as possible). A more

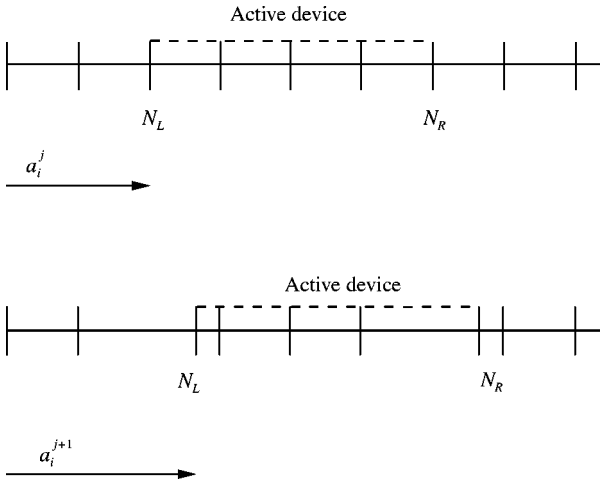

Figure 8. During an iteration, only the left and right outer nodes of the active device move (assuming that the length is constant).

interesting study would be to minimize the time response for the sensor outputs to vanish. As this criterion is not easy to use, one can decide to minimize the "mechanical energy integral" of the system with respect to the actuators design variables, called a_i: find a_i, $i = 1, \ldots$ which minimize

$$J_a(a_i) = \frac{1}{2T} \int_0^T \left\{ \frac{\mathrm{d}}{\mathrm{d}t} \{q_U\}^{\mathrm{T}} [M_{UU}] \frac{\mathrm{d}}{\mathrm{d}t} \{q_U\} + \{q_U\}^{\mathrm{T}} [K_{UU}] \{q_U\} \right\} \mathrm{d}t. \tag{14}$$

Also, the LQR method can be used to construct the control law; it consists in minimizing J_Φ given by equation (11) with respect to $\{q_\Phi\}_a$.

Thus, in the case of actuators, two optimization problems have to be solved simultaneously: the minimization of J_a with respect to a_i and the minimization of J_Φ with respect to $\{q_\Phi\}_a$. The control law depends especially strongly on the location of actuators. Consequently, it has been decided here to solve them iteratively. At each step of optimization of J_a, one minimizes J_Φ and keeps constant the corresponding matrix $[K]$.

3.3. THE OPTIMIZATION CRITERIA FOR SENSORS LOCATION

In the case of sensors, the optimal location of sensors is usually found by maximizing the energy of the system output J_y, as well as the contributions of individual modes to the output:

$$J_y = \frac{1}{2} \int_0^T \{y\}^{\mathrm{T}} \{y\} \, \mathrm{d}t.$$

When the system is released from the initial state $\{x\}(t = 0) = \{x_0\}$ without active damping ($\{q_\Phi\}_a = 0 \; t \geqslant 0$), the output energy is [7]

$$2J_y = \{x_0\}^{\mathrm{T}} [G_o(T)] \{x_0\},$$

where $[G_o(T)]$ is the observability gramian matrix

$$[G_o(T)] = \int_0^T \mathrm{e}^{[A]^{\mathrm{T}}t}[C]^{\mathrm{T}}[C]\ \mathrm{e}^{[A]t}\,\mathrm{d}t.$$

In the previous expression of J_y, only $[G_o(T)]$ depends on the sensors location. Also as initial conditions cannot be known, it is desirable to find the sensors location in such a way as to maximize some measure of the matrix $[G_o(T)]$ [7, 11].

In the case of neglected damping, and for T sufficiently large, $[G_o(T)]$ becomes diagonal dominant [7, 11]: i.e.,

$$[G_o](T) = \begin{pmatrix} \frac{1}{2}[\gamma]^2 & [0] \\ [0] & \frac{1}{2}[\gamma]^2 \end{pmatrix} T = [\tilde{G}_o]\,T,$$

where $[\gamma]$ is the diagonal matrix whose components for $i = 1, N$ are

$$\gamma_{ii} = \sum_{j=1}^{\bar{N}_s} C_{ji}^2 \quad \text{and} \quad [\tilde{G}_o] = \begin{pmatrix} \frac{1}{2}[\gamma]^2 & [0] \\ [0] & \frac{1}{2}[\gamma]^2 \end{pmatrix}.$$

Consequently, $2J_y = \{x_0\}^{\mathrm{T}}[\tilde{G}_o]\{x_0\}\,T$.

Several measures of $[G_o]$ can be used: its determinant, its trace or the product of the determinant with the trace. In order to ensure the observability of each mode, here it has been decided to use the first one. The optimization problem now is to find the parameters of the sensors location c_i, $i = 1, \ldots$ which minimize

$$J_s(c_i) = -\log(\det([\tilde{G}_o])) = -\sum_{i=1}^{N} \log(\lambda_i^2([\tilde{G}_o]))$$

$$= -\sum_{i=1}^{N} \log\left[\sum_{j=1}^{\bar{N}_s} ([K_{\Phi\Phi}]_s^{-1}[K_{\Phi U}]_s[\Psi][\omega]^{-1})_{ji}^2\right], \tag{15}$$

where λ_i are the eigenvalues of $[\tilde{G}_o]$. The logarithm function in equation (15) is used to decrease the value of the determinant of $[\tilde{G}_o]$.

3.4. THE OPTIMIZATION METHOD

In order to minimize the optimization criteria J_a and J_s, one can choose to use a gradient algorithm [18]. For optimizing a criterion $J(p)$, where p is the design parameter, this method consists in finding the solution p^* by constructing a sequence p^n such that

$$p^{n+1} = p^n - \varepsilon \frac{\partial J}{\partial p}(p^n), \qquad J(p^*) \leqslant J(p^{n+1}) \leqslant J(p^n), \qquad \lim_{n\to\infty} J(p^n) = J(p^*),$$

where ε is the step size of the algorithm. The use of this method needs the value of the derivative $\partial J/\partial p$. Then, the derivatives $\partial J_a/\partial a_i$ and $\partial J_s/\partial c_i$ have to be calculated.

As stated before, in this work, we did not want to consider constrained optimization in order to simplify the implementation of the algorithms. This is the reason why we search only one location for each optimization problem in the proposed examples.

4. DIFFERENTIATION OF THE TWO CRITERIA

4.1. ESTIMATION OF THE DERIVATIVES OF CRITERIA

In order to calculate derivatives, two methods can be used. The most common is the finite difference method, using the development

$$J(p + \Delta p) = J(p) + \frac{\partial J}{\partial p}\Delta p + o(p^2)$$

which becomes

$$\frac{\partial J}{\partial p} \simeq \frac{J(p + \Delta p) - J(p)}{\Delta p}.$$

This common method has several disadvantages: it needs the calculus of $J(p)$ and $J(p + \Delta p)$ which implies calculating one modal basis per parameter; it depends on the choice of Δp.

Thus, it is preferable here to differentiate the two criteria: this can be easily and systematically implemented in a finite element solver.

Let $\{\partial V/\partial p\}$ and $[\partial M/\partial p]$ be the derivatives of a vector $\{V\}$ and a matrix $[M]$ with respect to a scalar p:

$$\left\{\frac{\partial V}{\partial p}\right\} = \frac{\partial}{\partial p}\{V\}, \qquad \left[\frac{\partial M}{\partial p}\right] = \frac{\partial}{\partial p}[M].$$

With these notations, the derivative of J_a with respect to a_i is

$$\begin{aligned}\frac{\partial J_a}{\partial a_i} = \frac{1}{2T}\int_0^T \Bigg[& \left\{\frac{\partial \dot\alpha}{\partial a_i}\right\}^{\mathrm T}[\Psi]^{\mathrm T}[M_{UU}][\Psi]\{\dot\alpha\} + \left\{\frac{\partial \alpha}{\partial a_i}\right\}^{\mathrm T}[\Psi]^{\mathrm T}[K_{UU}][\Psi]\{\alpha\} \\ & + \{\dot\alpha\}^{\mathrm T}\left[\frac{\partial \Psi}{\partial a_i}\right]^{\mathrm T}[M_{UU}][\Psi]\{\dot\alpha\} + \{\alpha\}^{\mathrm T}\left[\frac{\partial \Psi}{\partial a_i}\right]^{\mathrm T}[K_{UU}][\Psi]\{\alpha\} \\ & + \{\dot\alpha\}^{\mathrm T}[\Psi]^{\mathrm T}\left[\frac{\partial M_{UU}}{\partial a_i}\right][\Psi]\{\dot\alpha\} + \{\alpha\}^{\mathrm T}[\Psi]^{\mathrm T}\left[\frac{\partial K_{UU}}{\partial a_i}\right][\Psi]\{\alpha\} \\ & + \{\dot\alpha\}^{\mathrm T}[\Psi]^{\mathrm T}[M_{UU}]\left[\frac{\partial \Psi}{\partial a_i}\right]\{\dot\alpha\} + \{\alpha\}^{\mathrm T}[\Psi]^{\mathrm T}[K_{UU}]\left[\frac{\partial \Psi}{\partial a_i}\right]\{\alpha\} \\ & + \{\dot\alpha\}^{\mathrm T}[\Psi]^{\mathrm T}[M_{UU}][\Psi]\left\{\frac{\partial \dot\alpha}{\partial a_i}\right\} + \{\alpha\}^{\mathrm T}[\Psi]^{\mathrm T}[K_{UU}][\Psi]\left\{\frac{\partial \alpha}{\partial a_i}\right\}\Bigg]\mathrm{d}t. \end{aligned} \tag{16}$$

Here, the model superposition (5) has been used. In the same way, the derivative of J_s with respect to c_i is

$$\begin{aligned}\frac{\partial J_s}{\partial c_i} = & -\sum_{k=1}^{N} 2\frac{1}{\sum_{j=1}^{\bar N_s}([K_{\Phi\Phi}]_s^{-1}[K_{\Phi U}]_s[\Psi][\omega]^{-1})_{jk}} \times \sum_{j=1}^{\bar N_s}\Bigg(\frac{\partial}{\partial c_i}[K_{\Phi\Phi}]_s^{-1}[K_{\Phi U}]_s[\Psi][\omega]^{-1} \\ & + [K_{\Phi\Phi}]_s^{-1}\left[\frac{\partial K_{\Phi U}}{\partial c_i}\right]_s[\Psi][\omega]^{-1} + [K_{\Phi\Phi}]_s^{-1}[K_{\Phi U}]_s\left[\frac{\partial \Psi}{\partial c_i}\right][\omega]^{-1} \\ & + [K_{\Phi\Phi}]_s^{-1}[K_{\Phi U}]_s[\Psi]\frac{\partial[\omega]^{-1}}{\partial c_i}\Bigg)_{jk} \times ([K_{\Phi\Phi}]_c^{-1}[K_{\Phi U}]_s[\Psi]'[\omega]^{-1})_{jk}. \end{aligned} \tag{17}$$

These two expressions show that $\partial J_a/\partial a_i$ depends on the derivatives of $\{\alpha\}$, $[\Psi]$, $[M_{UU}]$ and $[K_{UU}]$, and $\partial J_s/\partial c_i$ depends on the derivatives of $[\Psi]$, $[\omega]$, $[K_{\Phi\Phi}]_s$ and $[K_{\Phi U}]_s$. In the following sections it is shown how each of them can be calculated.

4.2. DERIVATION OF THE VARIABLE $\{\alpha\}$

The derivative $\partial\{\alpha\}/\partial a_i$ is obtained by differentiating the equations of motion (1) written in the modal basis, where $\{q_\Phi\}_a$

$$[q_\Phi\}_a = -[K]\{x\} = -[K_1]\{\alpha\} - [K_2]\{\dot{\alpha}\}.$$

As noticed previously, $[K]$ and consequently $[K_1]$ and $[K_2]$ are assumed to be constant for the calculation of $\partial J_a/\partial a_i$. Thus, $\partial\{\alpha\}/\partial a_i$ satisfies the equation

$$\begin{aligned}
&[\Psi]^{\mathrm{T}}[M_{UU}][\Psi]\left\{\frac{\partial\ddot{\alpha}}{\partial a_i}\right\} + [\Psi]^{\mathrm{T}}[K_{U\Phi}][K_2]\left\{\frac{\partial\dot{\alpha}}{\partial a_i}\right\} + [\Psi]^{\mathrm{T}}([K_{UU}][\Psi] + [K_{U\Phi}][K_1])\left\{\frac{\partial\alpha}{\partial a_i}\right\} \\
&= \left[\frac{\partial\Psi}{\partial a_i}\right]^{\mathrm{T}}\{F\} + [\Psi]^{\mathrm{T}}\left\{\frac{\partial F}{\partial a_i}\right\} \\
&\quad - \left(\left[\frac{\partial\Psi}{\partial a_i}\right]^{\mathrm{T}}[M_{UU}][\Psi] + [\Psi]^{\mathrm{T}}\left[\frac{\partial M_{UU}}{\partial a_i}\right][\Psi] + [\Psi]^{\mathrm{T}}[M_{UU}]\left[\frac{\partial\Psi}{\partial a_i}\right]\right)\{\ddot{\alpha}\} \\
&\quad - \left(\left[\frac{\partial\Psi}{\partial a_i}\right]^{\mathrm{T}}[K_{U\Phi}][K_2] + [\Psi]^{\mathrm{T}}\left[\frac{\partial K_{U\Phi}}{\partial a_i}\right][K_2]\right. \\
&\quad - \left(\left[\frac{\partial\Psi}{\partial a_i}\right]^{\mathrm{T}}[K_{UU}][\Psi] + [K_{U\Phi}][K_1]\right)\{\alpha\} \\
&\quad - [\Psi]^{\mathrm{T}}\left(\left[\frac{\partial K_{UU}}{\partial a_i}\right][\Psi] + [K_{UU}]\left[\frac{\partial\Psi}{\partial a_i}\right] + \left[\frac{\partial K_{U\Phi}}{\partial a_i}\right]\right)[K_1]. \qquad (18)
\end{aligned}$$

Note that the first part of the dynamical equation satisfied by $\partial\{\alpha\}/\partial a_i$ is the same as that of the equation satisfied by $\{\alpha\}$. It is only the second part which is different.

In the same way, the initial conditions are given by

$$\begin{aligned}
\left\{\frac{\partial\alpha}{\partial a_i}\right\}(t=0) &= \left[\frac{\partial\Psi}{\partial a_i}\right]^{\mathrm{T}}[M_{UU}]\{q_U\}(t=0) \\
&\quad + [\Psi]^{\mathrm{T}}\left[\frac{\partial M_{UU}}{\partial a_i}\right]\{q_U\}(t=0) + [\Psi]^{\mathrm{T}}[M_{UU}]\left\{\frac{\partial q_U}{\partial a_i}\right\}(t=0), \qquad (19) \\
\left\{\frac{\partial\dot{\alpha}}{\partial a_i}\right\}(t=0) &= \left[\frac{\partial\Psi}{\partial a_i}\right]^{\mathrm{T}}[M_{UU}]\{\dot{q}_U\}(t=0) \\
&\quad + [\Psi]^{\mathrm{T}}\left[\frac{\partial M_{UU}}{\partial a_i}\right]\{\dot{q}_U\}(t=0) + [\Psi]^{\mathrm{T}}[M_{UU}]\left\{\frac{\partial\dot{q}_U}{\partial a_i}\right\}(t=0). \qquad (20)
\end{aligned}$$

These equations depend on the derivatives of the matrices $[M_{UU}]$, $[K_{UU}]$ and $[K_{U\Phi}]$ and the derivatives of the eigenvectors.

4.3. DERIVATIVE OF EACH MATRIX, EIGENVECTORS AND EIGENVALUES

4.3.1. *Derivative of each matrix*

The derivative of each matrix ($[M_{UU}]$, $[K_{UU}]$, ...) can be determined by using the finite difference method detailed previously. In the finite element method, these global matrices are obtained by the summation of all corresponding element matrices. Each element matrix depends upon the location of the element nodes. The derivative of the matrix can then be numerically calculated with respect to any node co-ordinate and stored once and for all. If the location of these nodes is a known function of design parameters, it is very easy to get the derivative of any element matrix with respect to any design parameter by using the chain rule. Once this is done, the derivative of the global matrix is simply the summation of each element contribution.

In the case considered here, only the two end elements are taken into account for each active device (see Figure 8). The length L being constant, the co-ordinates x_L and x_R of the two end nodes N_L and N_R are connected to the same unique design parameter p concerning the device: $x_L = p$ and $x_R = p + L$, and thus $\mathrm{d}x_L/\mathrm{d}p = \mathrm{d}x_R/\mathrm{d}p = 1$. For a standard two-node beam, the derivative of associated matrices with respect to nodes co-ordinates can be obtained analytically by hand once and for all.

4.3.2. *Derivative of eigenvectors and eigenvalues*

The derivatives of the eigenvalues and eigenvectors with respect to a scalar p are obtained by using the usual sensitivity method developed in reference [18]. They are obtained by differentiating the equations of eigenvalue problems. Their expressions are

$$\frac{\partial(\omega_r^2)}{\partial p} = \{\Psi\}_r^{\mathrm{T}} \left(\frac{\partial [K]}{\partial p} - \omega_r^2 \frac{\partial [M]}{\partial p} \right) \{\Psi_r\}, \tag{21}$$

$$\frac{\partial \{\Psi_r\}}{\partial p} = \sum_{j=1}^{l} d_{rj} \{\Psi_j\} + \{\Psi_r\}^{\mathrm{S}} \quad \text{for } r = 1, \ldots N, \tag{22}$$

where

$$\{\Psi_r\}^{\mathrm{S}} = [K]^{-1} \left(\frac{\partial \omega_r}{\partial p} [M] - \frac{\partial [K]}{\partial p} + \omega_r^2 \frac{\partial [M]}{\partial p} \right) \{\Psi_r\} \text{ is a static correction term and}$$

$$d_{rj} = \frac{\omega_r^2}{\omega_j^2} \frac{1}{\omega_r^2 - \omega_j^2} \{\Psi_j\}^{\mathrm{T}} \left(\frac{\partial [K]}{\partial p} - \omega_r^2 \frac{\partial [M]}{\partial p} \right) \{\Psi_r\}, \quad r \neq j,$$

$$d_{rr} = -\frac{1}{2} \{\Psi_r\}^{\mathrm{T}} \frac{\partial [M]}{\partial p} \{\Psi_r\}, \tag{23}$$

with

$$l \in \mathbb{N}, \quad l \geqslant N.$$

The derivative of the eigenvector $\{\psi_r\}$ is decomposed in two parts: the first one is a decomposition in the truncated modal basis using the first l eigenvectors ($l > N$); the second one is a static correction term which accelerates the convergence. In the applications, the integer l has to be chosen sufficiently large.

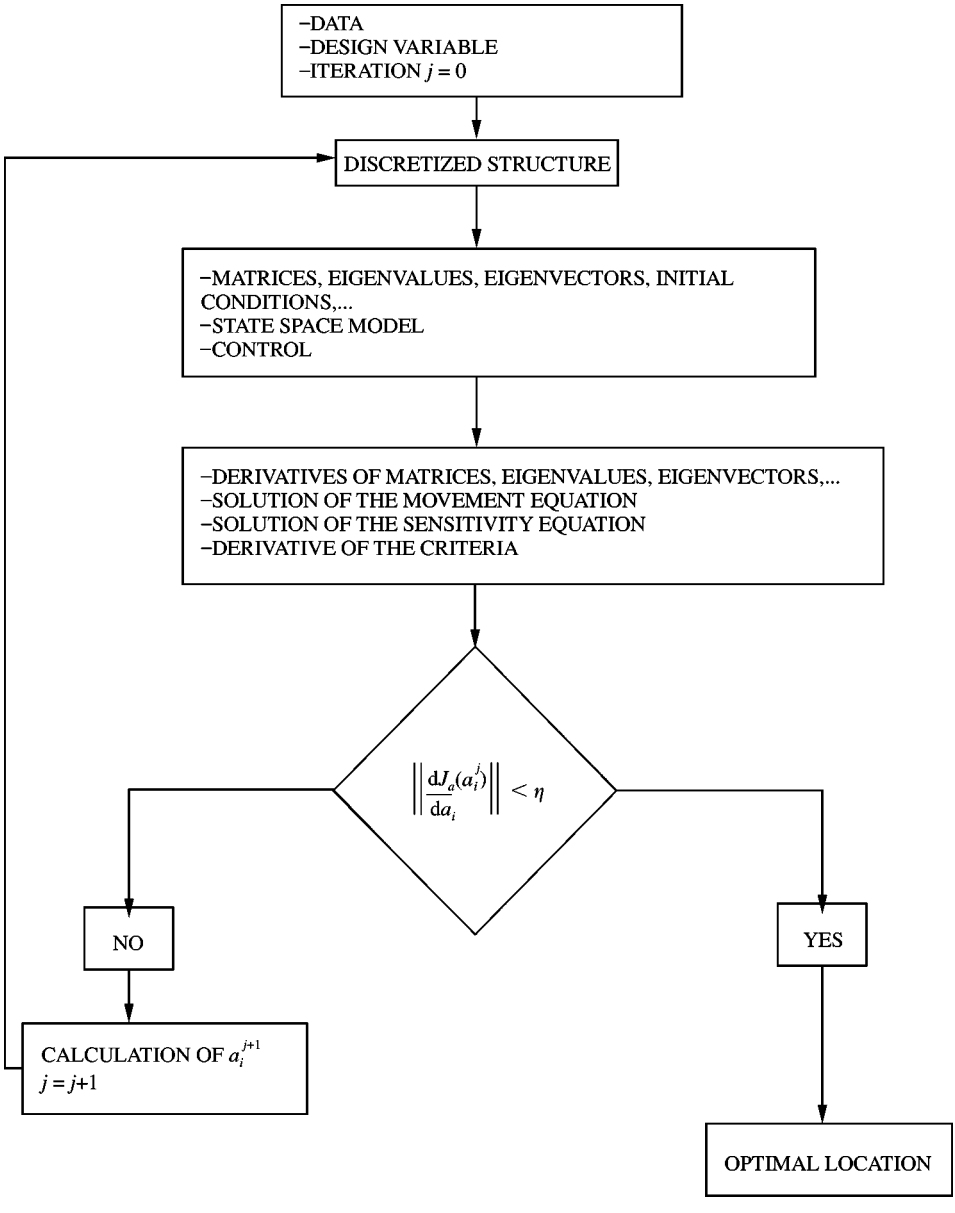

Figure 9. Algorithm for the actuator location.

5. APPLICATIONS

Here, the optimization algorithms are developed to find the optimal location of piezoelectric actuators and sensors on beam structures. Then, several applications are presented.

5.1. OPTIMIZATION ALGORITHMS

The two optimization algorithms are presented in Figures 9 and 10. They have been implemented in DYNANDID2D [16]. Each of them consists of three main steps: Step 1: the

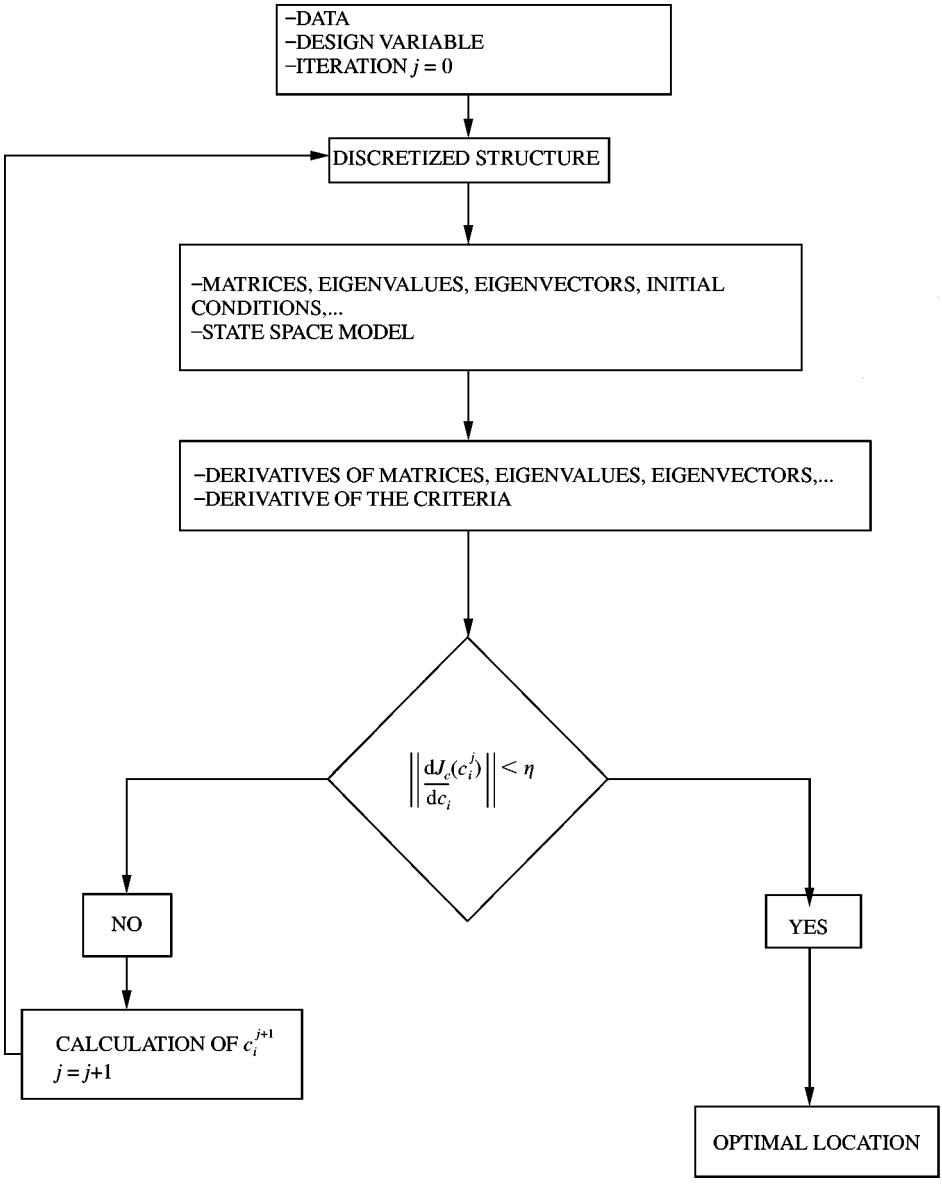

Figure 10. Algorithm for the sensor location.

reading of data; Step 2: the determination of the optimal solutions; Step 3: the study of the results.

More precisely, in the second step, the optimal locations are obtained iteratively. For iteration n, the structure location is defined by the design variables $\{a_i^n\}$ and the different steps are as follows:

- the construction of the geometrical discretization of the structure;
- the solution of the eigenvalue problem, and in the case of the optimization actuators location, the construction of the input voltage;

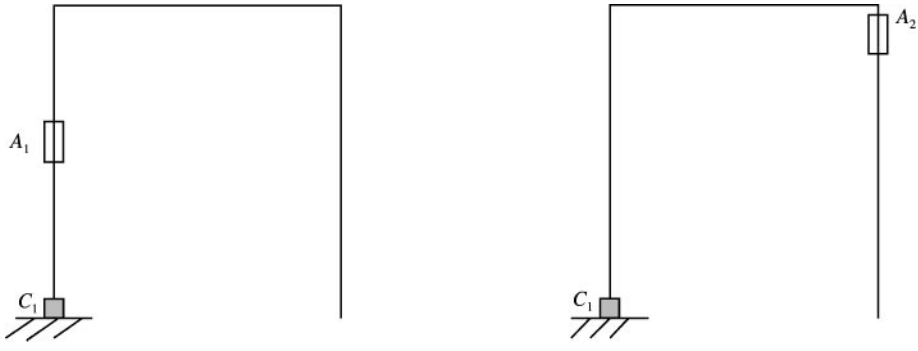

Figure 11. The two optimal locations of the actuator.

- the calculus of derivatives of matrices, eigenvalues and eigenvectors, and in the case of the optimization of actuators location, the solution of the equations of motion satisfied by $\{\alpha\}$ and $\partial\{\alpha\}/\partial a_i$;
- the calculus of the derivative of the criteria;
- the new design variables value: in the case of sensors location: $c_i^{n+1} = c_i^n - \varepsilon(\partial J_s/\partial c_i)(c_i^n)$, in the case of actuators location: $a_i^{n+1} = a_i^n - \varepsilon(\partial J_a/\partial a_i)(a_i^n)$.

For some design variables, the algorithm can find different optimal solutions. In this case, in order to keep only one of them, it is suggested to use several performance measures, for example the necessary time for sensor output to vanish. In the following sections, these two algorithms are used to find the optimal location of one actuator and one sensor on the three-beam structure and on a cantilever beam. Lengths of actuators and sensors are assumed to be constant.

5.2. THE THREE-BEAM STRUCTURE

In this section, the aim is to find the optimal location of the actuator and the sensor on the three-beam structure shown in Figure 2 and studied in section 2.3. The structure is again subjected to the release test. After several simulations, l used for the static correction term in equation (22) is taken to be equal to 8.

5.2.1 *Optimal location of the piezoelectric actuator*

The objective here is to find the optimal actuator location to stop the vibrations very quickly. The piezoelectric sensor is fixed at $C_1 = (0, 0)$.

Using the optimization algorithm for the actuators location, two local minima are found: $A_1 = (0{\cdot}00, 0{\cdot}22)$ and $A_2 = (0{\cdot}40, 0{\cdot}48)$ (see Figure 11). In order to stop the vibrations as quickly as possible for each case, the matrix $[R]$ in equation (11) is chosen to use a maximal voltage input [15]. Then, several performance measures can be used to find the best location between the two minima. Here, one can propose the following.

First, the homogeneity of the components of the vector $[K]$. The LQR method consists in using a control law like $\{q_\Phi\}_a = -[K]\{x\}$. As the control law must take into account the actual state of the structure as well as possible, the components of $[K]$ have to be homogeneous. For the two optima, the ratio $|\max_i K_i/\min_i K_i|$ is calculated. The second performance measure is the time required for sensor output to vanish.

TABLE 3

Determination of the optimal actuator location

Actuator location	A_1	A_2
$\left\lvert \frac{\max_i K_i}{\min_i K_i} \right\rvert$	8	20
Necessary time (s)	6	20

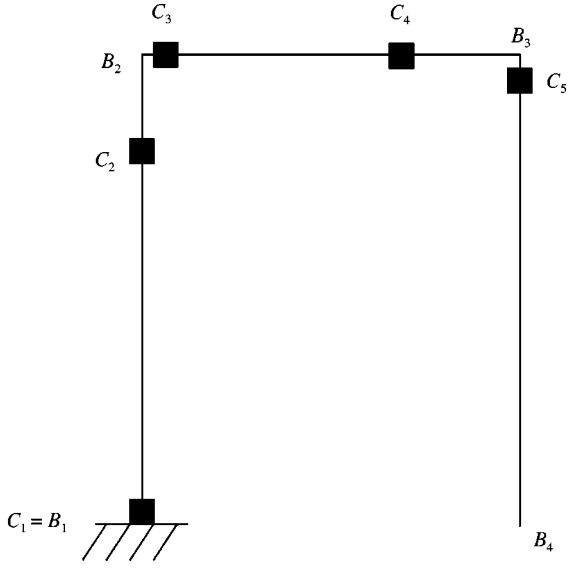

Figure 12. The optimal locations of the sensor.

From the results in Table 3 for the two performance measures, the first actuator location seems to be better than the second one. Consequently, it is considered as the optimal placement of the actuator in the case of the release test.

5.2.2. *Optimal location of the piezoelectric sensor*

In the same way, one can use the optimization sensors location algorithm to find the location of the piezoelectric sensor.

Five local minima are found: $C_1 = (0{\cdot}00, 0{\cdot}00)$, $C_2 = (0{\cdot}00, 0{\cdot}39)$, $C_3 = (0{\cdot}02, 0{\cdot}50)$, $C_4 = (0{\cdot}31, 0{\cdot}50)$ and $C_5 = (0{\cdot}40, 0{\cdot}48)$ (see Figure 12).

From the choice of the criterion J_s, these maxima are independent of the initial conditions. They ensure a good observability of all the modes, without especially taking into account the most excited modes.

In order to get an optimal location ensuring an efficient active control, one can propose, two performance measures.

The first one is the homogeneity of the components of the vector $[L]$. This vector balances the output in equation (12). Then its components have to be homogeneous to take into account the output of all modes. For each minimum, the ratio $|\max_i L_i / \min_i L_i|$ is calculated.

TABLE 4

Determination of the optimal sensor location

Sensor location	C_1	C_2	C_3	C_4	C_5
$\left\lvert \frac{\max_i L_i}{\min_i L_i} \right\rvert$	37	45	5·5	6·5	5·6
Necessary time (s)	6	10	10	10	6

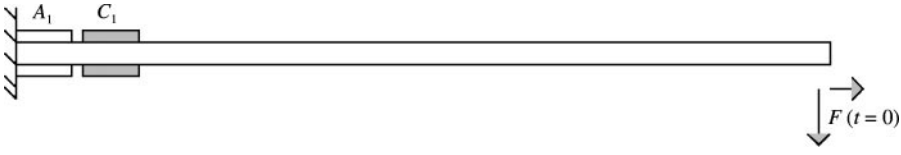

Figure 13. A cantilever beam.

TABLE 5

Characteristics of the simple cantilever beam

Length of the beam (m)	1
Length of the actuator and the sensor (m)	0·06
Width (m)	0·02
Thickness (m)	0·002
Mass density (kg/m^3)	2700
Young's modulus (Pa)	7×10^{10}
Natural frequencies (Hz)	1·64, 10·29, 28·81, 56·46

The second performance measure is the settling time of output. For each location, the settling time of the output to come back to the zero state using a piezoelectric actuator located in (0·001, 0·00), with maximal voltage input is determined.

Results are shown in Table 4. The location which seems to be the best for the two performance measures in C_5. Therefore, it is considered as the optimal location for the piezoelectric sensor in the case of release test.

The two optimization algorithms have been used to find the optimal location of one actuator and one sensor on a three-beam structure. Results show that these optimal locations are not obviously defined. Also, they depend on the nature of the disturbance applied to the structure. In the next section, the number of actuators and sensors needed in the case of a cantilever beam is discussed.

5.3. A CANTILEVER BEAM

In this section, a simple cantilever beam is considered, whose length is 1 m (see Figure 13). The geometrical and mechanical characteristics of the system are detailed in Table 5. Again the first four modes are taken into account and l is to taken to be equal to 8.

TABLE 6

Determination of the optimal sensor location on the beam

Sensor location (m)	0	0·081	0·146	0·258	0·393	0·533	0·684
$\left\lvert \frac{\max_i L_i}{\min_i L_i} \right\rvert$	20	5	100	10	35	20	8
Necessary time (s)	2·4	2·3	2·35	2·5	2·5	2·8	3·8

TABLE 7

The optimal location of the second actuator

Location of the second actuator (m)	0·17	0·78
$\left\lvert \frac{\max_i K_i}{\min_i K_i} \right\rvert$	21	157
Necessary time (s)	2·2	3·3

5.3.1. *Optimal location for one actuator and one sensor*

In the same way as in the previous section, the optimal locations of one actuator and one sensor are determined when the vibrations come from a release test ($F(t = 0) = 0{\cdot}003$ N applied at the endpoint). In the case of the actuator, the optimization algorithm gives only one minimum: at the field end A_1. In the case of the sensor, seven local minima are obtained (see Table 6). Using the two previous performance criteria, the optimal location of the sensor is $C_1 = 0{\cdot}081$ m (see Figure 12).

These locations are optimal in the case of the release test.

5.3.2. *Optimal location for a second actuator and a second sensor*

Consider now the situation where a first optimization has been done to get good behaviour in the case of the release test. The configuration is kept and one can consider the response of the active system to another kind of loading: i.e., a sinusoidal load equal to $F(t) = 0{\cdot}06 \cos(80t)$, whose period is T_e is applied at the beam end. As the load is harmonic, the final time T in equation (14) is chosen equal to $N_e T_e$. $N_e \in \mathbb{N}$ is such that for $t = T$ the system is in steady state. For the optimal configuration (see Figure 13) the system reaches steady state in 3·9 s. In order to increase the efficiency of the control when a sinusoidal load is applied to the beam, one can put another actuator and another sensor on the beam. In this way, one can consider the first actuator and sensor locations, called A_1 and C_1, as fixed and use again the two optimization algorithms to locate the second actuator and the second sensor (locations called A_2 and C_2). This can be considered as an optimal improvement of the unchanged first choices.

The algorithm used for the second actuator location gives two minima (see Table 7). Using the first performance criterion detailed previously and the necessary time for the system to reach steady state, the optimal location for the second actuator is $A_2 = 0{\cdot}17$ m. Then, with the two actuators, the system reaches steady state in less than 2·2 s. In the same

TABLE 8

Determination of the second sensor location

Location of the second sensor (m)	0·060	0·240	0·485	0·720
$\left\lvert \frac{\max_i L_i}{\min_i L_i} \right\rvert$	3·5	19	18·5	36
Necessary time (s)	2·4	2·5	2	2·8

way, using the optimization algorithm for sensors, one obtains four local minima for the second sensor location (see Table 8). The performance measures give $C_2 = 0{\cdot}485$ m as the optimal location for the second sensor. In this case, the system reaches steady state in 2 s.

Consequently, adding one actuator and one sensor gives a more efficient active control in the case of a sinusoidal load. As the first actuator and sensor locations have not changed, the active control system is also efficient for the release test.

The optimal additional sensors and actuators locations have been obtained for considering successively, and in a given order, two particular loading conditions, release test and sinusoidal load. It is clear that this process does not lead to the solution of finding optimal locations of two actuators (or sensors) for both release test and sinusoidal load: this would imply considering simultaneously the two loadings and moving simultaneously two actuators (and two sensors).

6. CONCLUSIONS

In this paper, a new approach is proposed to find the optimal location of piezoelectric actuators and sensors on structures. In order to simplify the optimization problem, it has been decided to search independently for the optimal locations of actuators and sensors. The first ones are obtained by minimizing the mechanical energy integral of the system and the second one by maximizing a measure of the gramian observability. This method is based on the differentiation of the optimization criteria and equations of motion with respect to the design variables.

In order to test the feasibility of the proposed method, the implemented optimization algorithm was limited to only one design variable and could not take into account constraints. This is the reason why only optimizations dealing with one parameter at a time have been shown.

Optimal locations (or optimal new locations) are obtained for a given loading condition. It is clear that the choice of this loading has, *a priori*, a significant influence on the results. This could be studied in future to show the sensitivity of the result to this choice.

This methodology has been developed here for beam structures by using results of reference [12]. As it is implemented in an FEM code, some results are directly usable for more complex structures, and the methodology can be extended to these cases.

Also, a new problem arises: how many actuators and sensors are necessary to have effective active control?

REFERENCES

1. S. M. YANG and Y. J. LEE 1993 *Journal of Smart Materials Structures* **2**, 96–102. Optimization of non-collocated sensor/actuator location and feedback gain in control systems.

2. C. R. FULLER, S. J. ELLIOTT and P. A. NELSON 1996 *Active Control of Vibration*. New York: Academic Press.
3. A. PREUMONT 1997 *Vibration Control of Active Structures. An Introduction*. Dordrecht: Kluwer Academic Publishers.
4. A. BLANGUERNON, F. LÉNÉ and M. BERNADOU 1999 *Journal of Smart Materials Structures* **8**, 116–124. Active control of a beam using a piezoelectric element.
5. I. BRUANT 1999 *Ph.D. Thesis, ENS Cachan France*. Positionnement optimal d'actionneurs et de capteurs en contrôle actif des vibrations de structures, application à des poutres équipées d'éléments piézo-électriques.
6. A. ARBEL 1981 *International Journal of Control* **33**, 565–574. Controllability measures and actuator placement in oscillatory systems.
7. A. HAC and L. LIU 1993 *Journal of Sound and Vibration* **167**, 239–261. Sensor and actuator location in motion control of flexible structures.
8. S. DEVASIA, T. MERESSI, B. PADEN and E. BAYO 1993 *Journal of Guidance, Control and Dynamics* **16**, 859–864. Piezoelectric actuator design for vibration suppression: placement and sizing.
9. A. K. DHINGRA and B. H. LEE 1995 *International Journal for Numerical Methods in Engineering* **38**, 3383–3401. Multiobjective design of actively controlled structures using a hybrid optimization method.
10. S. KONDOH, C. YATOMI and K. INOUE 1992 *JSME International Journal Series* 3 **33**,145–152. The positioning of sensors and actuators in the vibration control of flexible systems.
11. H. BARUH 1992 *Control and Dynamic Systems* **52**, 359–390. Placement of sensors and actuators in structural control.
12. I. BRUANT, G. COFFIGNAL, F. LÉNÉ and M. VERGÉ 1999 *Proceedings of the Conference Active*'99, *Fort Lauderdale*, 327–328. Optimal location of piezoelectric actuators on beam structures.
13. M. GÉRADIN and D. RIXEN 1992 *Théorie des Vibrations, Application à la Dynamique des Structures*. Paris: Masson.
14. T. KAILATH 1980 *Linear Systems*. Englewood Cliffs, NJ: Prentice-Hall.
15. I. BRUANT, G. COFFIGNAL, F. LÉNÉ and M. VERGÉ 1997 *Proceedings of the Conference Active* '97 *Budapest*, 635–648. Optimal location of piezoelectric actuators on a beam.
16. DYNADID2D G. COFFIGNAL 1996 LMS Paris ENSAM Code de calcul en éléments finis de poutres.
17. SCILAB Software 1996 INRIA Unité de Recherche de Rocquencourt-project Meta2, France.
18. R. T. HAFTKA and Z. GURDAL 1993 *Elements of Structural Optimization*. Dordrecht: Kluwer Academic Publishers.